

PRELIMINARY DESIGN ASSESSMENT OF THE MOLTEN SALT FAST REACTOR

E. MERLE-LUCOTTE, D. HEUER, M. ALLIBERT, M. BROVCHENKO, V. GHETTA,
A. LAUREAU, P. RUBIOLO

LPSC-IN2P3-CNRS / UJF / Grenoble INP, 53 rue des Martyrs, F-38026 Grenoble Cedex, France

ABSTRACT

In the frame of developing future energy resources and reducing nuclear wastes, the molten salt reactor concept offers very good potential. Molten salt reactors are liquid fuel reactors so that they are flexible in operation but very different in the design and safety approach compared to solid-fuelled reactors. This paper will address design issues of the MSFR, detailing some technological choices for the system components (fuel salt composition and distribution, core geometry, fuel heat exchangers...).

1. Introduction

Starting from the Oak-Ridge Molten Salt Breeder Reactor prototype, parametric studies were performed, focusing on breeding capabilities, reprocessing requirements, safety issues and more recently on nuclear power plant design, resulting in an innovative breeder concept: the Molten Salt Fast Reactor or MSFR [1-6]. The MSFR, with a fast neutron spectrum and operated in the Thorium fuel cycle, may be started with ^{233}U , enriched U, and/or TRU elements as initial fissile load. This concept has been recognized as a long term alternative to solid-fuelled fast neutron systems with a unique potential (large negative temperature and void coefficients, lower fissile inventory, no initial criticality reserve, simplified fuel cycle, wastes reduction...) and is thus one of the reference reactors of the Generation IV International Forum [7].

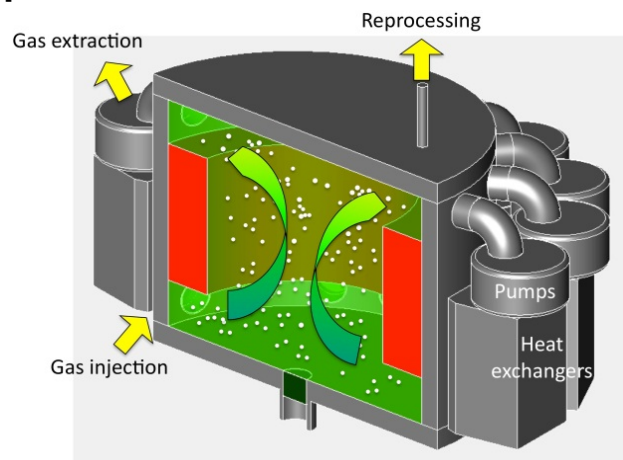


Fig.1: Schematic conceptual MSFR design

The reference MSFR is a 3000 MWth reactor with a total fuel salt volume of 18 m³, operated at a mean fuel temperature of 750°C. Figure 1 sketches the general component outlines for such a MSFR. The core consists of a circulating fluoride salt loaded with the fuel (note the absence of solid matter in core). The fuel salt considered in the simulations is a binary fluoride salt with 77.5% of lithium fluoride; the other 22.5% are a mix of heavy nuclei fluorides. This proportion, set throughout the reactor evolution, leads to a fast neutron spectrum. The total fuel salt volume is distributed half in the core and half in the external fuel circuit. This MSFR system thus combines the generic assets of fast neutron reactors (extended resource utilization, waste minimization) with those associated to a liquid-fuelled reactor.

In preliminary designs developed in relation to calculations, the core of the MSFR is a single compact cylinder (2.25m high x 2.25m diameter) where the nuclear reactions occur within the liquid fluoride salt acting both as fuel and as coolant. The external core structures and the fuel heat exchangers are protected by thick reflectors made of nickel-based alloys, which have been designed to absorb more than 99% of the escaping neutron flux. These reflectors

are themselves surrounded by a 20cm thick layer of B_4C , which provides protection from the remaining neutrons. The radial reflector includes a fertile blanket (50 cm thick - red area in Fig. 1) to increase the breeding ratio. This blanket is filled with a fertile salt of $LiF-ThF_4$ with initially 22.5mole % $^{232}ThF_4$.

The return circulation of the salt (from the top to the bottom) is divided into 16 groups of pumps and heat exchangers located around the core [8]. The neutronic reflectors, made of NiCrW-based alloy, constitute the lower and upper walls of the core. The lower reflector is connected to a draining system: in case of a planned shut down or incident/accident leading to a temperature increase in the core, the fuel configuration may be changed passively by gravitational evacuation of the fuel salt in tanks located under the reactor where a passive cooling will be achieved.

Conceptual design activities are currently underway so as to increase the confidence that MSFR systems can satisfy the goals of Generation-IV reactors in terms of sustainability (Th breeder), non proliferation (integrated fuel cycle, multi-recycling of actinides), resource savings (closed Th/U fuel cycle, no uranium enrichment), safety (no reactivity reserve, strongly negative feedback coefficient) and waste management (actinide burner). Two of these studies related to the fuel salt are detailed in this paper. The selection of the liquid fuel composition is presented in the second section, based on neutronics, materials and chemical considerations. The third section presents the global method developed to assess the design of the heat exchangers while taking into account the requirements of the entire fuel circuit, since the fuel salt is also used as the coolant in such reactors. One of the main constraints on the design of the fuel circuit of the MSFR is indeed the ability to evacuate the heat generated while restraining the fuel salt volume mobilized out of the core for this task.

2. Which liquid fuel?

The use of a liquid fuel has significant potential benefits:

- The homogeneity of the fuel allows uniform combustion, thereby avoiding loading plans
- Fuel management involves only fluid transfers
- Reprocessing and fuel preparation require no change of state
- In an emergency, the fuel can be transferred quickly by gravitational flow to vessels designed to evacuate the residual power passively
- Fuel reprocessing can be done online or in batch mode on discrete samples and therefore without requiring reactor shutdown.

Liquid-fuelled reactors are « homogeneous reactors » that have intrinsic safety properties thanks to the fuel's expansion coefficient that induces large negative thermal and void feedback coefficients. Because of this, such reactors can be controlled without control or command rods.

The choice of liquid fuel is guided by operational considerations, but also the need to meet the GEN IV recommendations. The main criteria are:

- A melting temperature not too high and a sufficiently high boiling point
- Low vapour pressure
- Good thermal and hydraulic properties
- Good stability under irradiation
- Sufficient solubility of fissile and fertile elements
- Avoid the production of unmanageable radioisotopes
- A high neutron transparency
- An identified fuel reprocessing method.

Taking into account all these constraints, the choice is reduced to two possible types of liquid: a fluoride or a chloride salt. We thus compare in this paper the characteristics of a MSFR operated in the Thorium fuel cycle while using fluoride or chloride salts. Two fuel salts have been considered in our reactor simulations: $LiF-(HN)F_4$ with 22.5% heavy nuclei (HN), and $NaCl-(HN)Cl_4$ with 28% heavy nuclei. Both salt compositions correspond to eutectic points of their respective phase diagram, with a melting temperature respectively of 565°C (fluoride

salt) and 375°C (chloride salt). More precisely, we have considered a fluoride salt enriched in ^7Li (99.999 % of ^7Li and 0.001% of ^6Li) and a chloride salt enriched in ^{37}Cl (99% of ^{37}Cl and 1% of ^{35}Cl), at the feasibility limit in both cases.

Considering only the chemical characteristics of the salts is not discriminatory, each salt having its own drawbacks / advantages. For example, the reference technique to extract U and Pu is fluorination, without a corresponding process for a chloride mixture. The actinide solubility is higher in chloride than in fluoride salts, which could be a limiting factor to start a MSFR with actinide elements. On the other hand, the boiling temperature of chloride salts is 300°C lower than that of the fluoride salts (respectively around 1400°C and 1700°C), which would have to be taken into account in safety studies for transient analyses.

We now compare chloride and fluoride salts according to neutronics considerations.

2.1 Breeding capabilities and irradiation damages

The neutronic characteristics of a MSFR, based on the Thorium fuel cycle, and using a chloride / fluoride fuel salt, are listed in Tab 1. These results have been obtained via full numerical simulations of each system.

Parameter	Fluoride Salt	Chloride Salt
Thorium capture cross-section σ_C^{Th} in core (barn)	0.61	0.315
Thorium amount in core (kg)	42 340	47 160
Thorium capture rate in core (mole/day)	11.03	8.48
Thorium capture cross-section σ_C^{Th} in blanket (barn)	0.91	0.48
Thorium amount in the blanket (kg)	25 930	36 400
Thorium capture rate in the blanket (mole/day)	1.37	2.86
^{233}U initial inventory (kg)	5720	6867
Neutrons per fission ν in core	2.50	2.51
^{233}U capture cross-section $\sigma_C^{^{233}\text{U}}$ in core (barn)	0.495	0.273
^{233}U fission cross-section $\sigma_f^{^{233}\text{U}}$ in core (barn)	4.17	2.76
Capture/fission ratio α (spectrum-dependent)	0.119	0.099
Total breeding ratio	1.126	1.040

Tab. 1: Neutronic characteristics of the MSFR

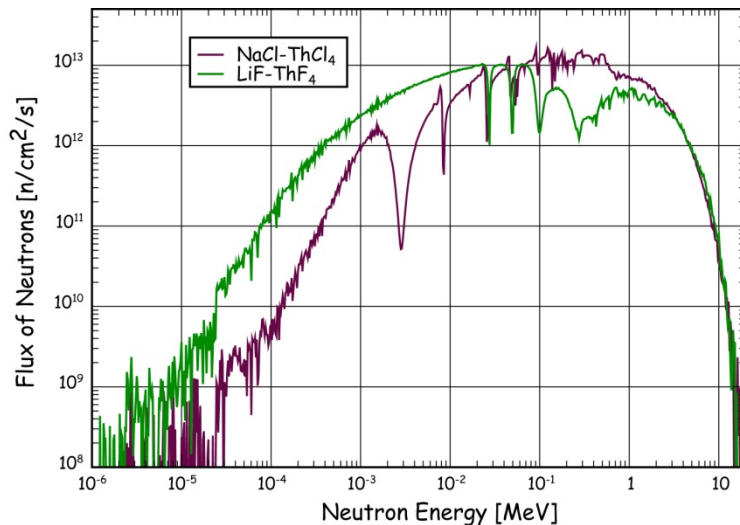


Fig 2. Neutron Spectra for a chloride (purple curve) and a fluoride (green curve) salt in a MSFR

The salt density is equal to 4.1 for the fluoride salt and to 3.2 for the chloride salt. The chloride salt is consequently more transparent to neutrons, and, with an identical reprocessing (typically some ten litres of fuel salt per day), breeding is obtained only with a larger chloride salt volume of around 40 m³ in the core and 20 m³ in the fertile blanket, instead of respectively around 20 m³ and 8 m³ for a fluoride salt. This transparency to neutrons is probably due not only to the lower density of the chloride salt, but also to the absence of inelastic scattering on Cl as compared to F. The neutron spectrum is thus faster in the chloride salt (cf. Fig. 2) and neutrons have a smaller probability of interaction. The mean capture cross-section on Thorium is thus equal to 0.61 barn in the fluoride salt and to 0.315 barn only in the chloride salt. As the amounts of Thorium in each case are quite similar, the capture rate on Thorium in the fluoride salt is more important (11.03 mole/day) than that in the chloride salt (8.48 mole/day).

We can easily evaluate the ratio of the breeding rates in the two systems, assuming that all the fissions occur on ²³³U and that the ²³³Pa does not capture.

The reactivity is then equal to: $k = \frac{\nu \tau_f^{233U}}{\tau_{Abs}^{All}} = 1$

with τ_X^Y the reaction rate X on the nucleus Y and ν the number of neutrons produced per fission. The breeding ratio is then equal to:

$$R = \frac{\tau_c^{Th}}{(1 + \alpha) \tau_f^{233U}} = \frac{\nu \tau_c^{Th}}{(1 + \alpha) \tau_{Abs}^{All}}, \alpha \text{ being the ratio } \frac{\sigma_c^{233U}}{\sigma_f^{233U}}.$$

Noting that the total absorption rate is identical in both cases since the total powers are equal, we deduce the ratio of the breeding rates in MSFRs based on fluoride and chloride salts:

$$\frac{R_{Cl}}{R_F} = \frac{\nu_{Cl} (1 + \alpha_F) (\tau_c^{Th})_{Cl}}{\nu_F (1 + \alpha_{Cl}) (\tau_c^{Th})_F} = 0.935$$

This ratio calculated with a full simulation of both systems is equal to $\frac{1.04}{1.126} = 0.924$

As a conclusion, the breeding ratio of a MSFR operated with a chloride salt is clearly degraded as compared to that of a MSFR operated with a fluoride salt, in spite of the fact that the chloride salt volume considered is twice that of the fluoride salt.

Finally, the radiation damages in neutron-irradiated materials, dependent on many factors like the irradiation dose and the neutron spectrum, and expressed in dpa (displacements per atom), is directly impacted by the choice of the salt. Our calculations show that, in the most irradiated area corresponding to the first two centimetres of the central area (radius 20 cm and thickness 2 cm) of the axial reflector, the damages are 4 times higher (30 dpa/year against 7.5 dpa/year) for the chloride salt compared to the fluoride salt. This is due to the chloride salt neutron spectrum which is faster than that of the fluoride salt (see Fig. 2).

2.2 Production of problematic elements

The presence of Cl in the salt leads to the production of ³⁶Cl, whose radioactive period is 301 000 years. This element is very mobile, it is thus impossible to confine it over such large periods. ³⁶Cl is produced through two production modes: ³⁵Cl(n,γ)³⁶Cl and ³⁷Cl(n,2n)³⁶Cl. The first mode is far more probable, requiring a salt enriched in ³⁷Cl. Although we have chosen a significant enrichment of 99%, the first mode is still dominant with a production of ³⁶Cl of around 10 moles per year (360 grams/year, with a total production of 373 grams/year). This production can be compared with the production of Tritium in the case of the Lithium fluoride salts, which amounts to 55 moles/year (166 grams/year). However the Tritium, also mobile, has a radioactive period of 12 years only, being thus truly less problematic. This ³⁶Cl production represents one of the major drawbacks of chloride salts.

Finally the presence of Cl in the salt also leads to the production of Sulphur, mainly through the reactions ³⁷Cl(n,α)³⁴P(β-[12.34s])³⁴S and ³⁵Cl(n,α)³²P(β-[14.262 days])³²S. Even with the

large enrichment of 99% in ^{37}Cl , these reactions produce very large amounts of Sulphur in the salt (around 10 moles/year). This sulphur production has to be compared with the production of Oxygen in the fluoride salt, via the reaction $^{19}\text{F}(n,\alpha)^{16}\text{O}$, which amounts to 88.6 moles/year. In both cases, the element produced is very corrosive. But, while the Oxygen corrosion only affects the surface of metals, Sulphur weakens metals by placing itself on the grain boundaries, being thus much more corrosive. However, as both Oxygen and Sulphur will form compounds with some fission products, the proportion of these elements contributing to the corrosion of the structural materials is not really known. The Sulphur production has also to be compared to the production of Tellurium, which amounts to 200 moles/year in both fluoride and chloride salts. The corrosion mechanisms due to Tellurium and Sulphur are similar, so that the Sulphur production, which is significantly smaller than that of Tellurium does not represent a major drawback of chloride salts.

3. Conceptual design of the heat exchangers

One of the main constraints on the design of the fuel circuit of the MSFR is the ability to evacuate the heat generated while restraining the fuel salt volume mobilized for that task. Upon exiting the core, the fuel salt travels through a liquid-gas separator, a pump, a heat exchanger and returns to the core's bottom inlet. The circuit must bypass the fertile blanket and the neutron protections while taking the shortest route so as to minimize the fuel salt volume within these components. Since here the fuel salt also plays the role of the coolant, the dimensioning of the heat exchangers is constrained by the requirement that the heat evacuation is to mobilize the minimal fuel salt volume. Examples of such dimensioning solutions are given in this section to illustrate the problem.

3.1. Characterization of the heat exchanges

Suppose a plate heat exchanger made of Hastelloy and where the fuel salt and the intermediate fluid circulate in opposite directions on either side of a set of plates, as illustrated in Fig 3.

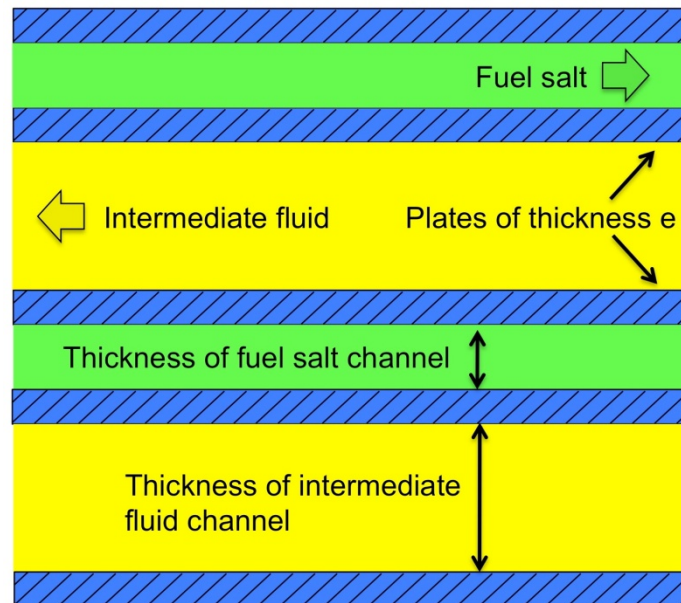


Fig 3. Schematic longitudinal view of the heat exchangers considered in this modeling

The heat exchange involves 2 thermal exchange coefficients (h_c for the fuel salt, h_i for the intermediate fluid) and the thermal resistance of the plate R_p , defined by:

$$h_{c,i} = \frac{\lambda Nu}{D} \quad \text{and} \quad \frac{1}{R_p} = \frac{\lambda}{e}$$

where λ is the fluid's or plate's thermal conductivity, D the hydraulic diameter, e the thickness of the plate or the equivalent static thickness of the fluid, Nu the Nusselt Colburn dimensionless number defined, via the Reynolds (Re) and the Prandtl (Pr) numbers, by the following equations (for $Pr > 0.5$):

$$Nu = 0.023 Re^{4/5} Pr^{1/3} \quad Re = \rho V D / \mu \quad Pr = C_p \mu / \lambda \quad \text{and} \quad D = 4s/p$$

With: ρ the mass density, V the flow speed, μ the dynamic viscosity, C_p the heat capacity, s the flow section, and p the perimeter of this flow section.

For $Pr \ll 1$ (liquid metals), the Nu number is calculated by:

$$Nu = b.Re^m$$

with b and m depending upon the Pr number as listed in [9].

The overall heat exchange coefficient is then obtained as:

$$\frac{1}{h} = \frac{1}{h_c} + R_p + \frac{1}{h_i}$$

Given the power P to be extracted and the mean temperature difference ΔT between the two heat transfer fluids, the necessary exchange surface is calculated as follows: $S = P/h.\Delta T$

The salt volume that can be mobilized in the heat exchangers being fixed, the gap between the plates (also called thickness of the fuel salt channel in the following) is predetermined so that the hydraulic diameter can be calculated recursively so as to re-determine the overall heat exchange coefficient h . It is then possible to derive the pressure drop in the exchangers as well as in the pipes that convey the fuel salt from the core to the exchangers and from the exchangers back to the core using the following relationships:

$$\Delta P = \frac{1}{2} L \Lambda \rho V^2 / D \quad \text{with} \quad \Lambda^{1/2} = -1.8 \text{Log} \left[6.9 / Re + (\epsilon / (3.7 D))^{1.11} \right]$$

With L the pipe's length and Λ a pressure drop coefficient calculated using the Colebrook equation approximated by Haaland for the turbulent case, the roughness of the pipe surface ϵ is taken equal to 10^{-5} . The singular pressure drops in the pipes due to the bends have been added, equal to $\frac{1}{2} \kappa \rho V^2$ per bend where κ is the pressure drop coefficient equal to 0.35 for a bend of 90° .

3.2 Physicochemical properties of the fluids

The initial fuel salt is composed of ${}^7\text{LiF}-\text{ThF}_4$ (20 mole%) - ${}^{233}\text{UF}_3$ (2.5 mole%) with 77.5 mole % of LiF , this fraction being kept constant during reactor operation. The fraction of ${}^{233}\text{U}$ is adjusted initially to have an exactly critical reactor. During reactor operation, fission products and new heavy nuclei are produced in the salt up to some mole % only, they do not impact the salt physicochemical properties needed for our studies. We have used the characteristics of the initial fuel salt [10], as presented in Table 2. The melting temperature of the fuel salt is equal to 565°C . The linear increase of the calorific capacity is limited to 800°C .

		Unit	Formula	A	B
Calorific capacity	C_p	J/K/kg	A+BT	-1111	2,78
Thermal Conductivity	λ	W/K/m	A+BT	0.928	8.40E-05
Density	ρ	kg/m ³	A+BT	4983.56	-0.882
Dynamic viscosity	μ	Pa.s	$\rho .A.\exp(B/T)$	5.55E-08	3689

Tab. 2: Physicochemical properties of the fuel salt as a function of its temperature T in K [10]

The physicochemical properties used for the three intermediate fluids considered here are summarized in Table 3. The exact composition of the fluid labelled « FLiNaK » is LiF (46.5 mole%) - NaF (11.5 mole%) - KF (42 mole%). The composition of the salt labelled « $\text{NaF} - \text{NaBF}_4$ » is: NaF (8mole%) - NaBF_4 (92 mole%). For the liquid lead, the maximal temperature at the surface, in contact with the structural materials, has been limited to 530°C to limit the corrosion rate, if it takes place.

		Unit	Liquid lead	FLiNaK	NaF-NaBF ₄
Calorific capacity	C _p	J/K/kg	175.1 - 4,96.10 ⁻² .T + 1,99.10 ⁻⁵ .T ² - 2.10.10 ⁻⁹ .T ³ - 1.52.10 ⁶ .T ²	976.199 + 1.0624.T	1506
Thermal Conductivity	λ	W/K/m	9.2 + 0.011.T	0.36 + 5.60.10 ⁻⁴ .T	0.66 - 2.37.10 ⁻⁴ .T
Density	ρ	kg/m ³	11367-1.1944.T	2579.3 - 0.624.T	2446.3 - 0.711.T
Dynamic viscosity	μ	Pa.s	4.55.10 ⁻⁴ . exp(1069/T)	2.49.10 ⁻⁵ . exp(4476.23/T)	8.77.10 ⁻⁵ . exp(2240/T)
Melting temperature	T _m	°C	327	454	384

Tab. 3: Physicochemical properties of the intermediate fluids [11,12,13]
(with T the temperature of the fluid in K)

3.3 Analytical method and typical solutions

A global geometry can be found by setting some parameters and constraints. A configuration that best satisfies these constraints can then be sought by adjusting a list of variable design parameters.

The preset parameters, evaluated through previous neutronic studies of the reactor core are:

- the total power is set at 3GW_{th}
- the core diameter is equal to the core height
- there are 16 identical sectors comprising a liquid-gas separator, a pump and a heat exchanger as well as any joining pipes
- the fuel salt volume is 18 m³, 50 % of it in core, 5 % in auxiliary volumes (overflow tank, spaces, etc.) and 45 % in the liquid-gas separators, the pumps and pipes, the heat exchangers
- the fertile blanket thickness is 500 mm and the neutron protection thickness is 200 mm

Other secondary parameters are prefixed as well, to simulate the liquid-gas separators, the heat exchanger inputs-outputs, the isolated pressure losses (bends, liquid-gas separators), and the pipes conveying the intermediate fluid to the exchangers. This analytical method has been applied for three intermediate fluids: liquid lead and two salts with a melting point lower than that of the fuel salt (LiF-NaF-KF and NaF-NaBF₄).

The variable parameters of the present studies are:

- the diameter of the pipes
- the thickness of the plates
- the gap between the plates on the intermediate fluid side, also called "thickness of the intermediate fluid channel" in this paper
- the fuel salt temperature at core entrance
- the fuel salt temperature increase within the core
- the temperature increase of the intermediate fluid in the heat exchangers
- the mean temperature difference between the two fluids within the heat exchangers

Some parameters are constrained to ensure an acceptable mode of operation. The most important ones are listed in table 4 along with their limiting value and acceptable deviation.

Each set of values of the variable parameters is evaluated using the following quality function:

$$\prod_i \exp\left(\frac{P_i - P_{0i}}{\sigma_i}\right)$$

where P_i is the value of the i^{th} parameter, P_{oi} the limiting value of the parameter, and σ_i the acceptable deviation for the parameter. The set of values of the variable parameters that minimizes this function is then sought. Typical results are shown in table 5 for the three intermediate fluids considered here.

Constrained Parameter	Limiting value (P_{oi})	Acceptable deviation (σ_i)
Minimum thickness of the fuel salt channel	2.5 mm	0.05 mm
Minimum thickness of the plate	1.75 mm	0.035 mm
Maximum speed of the fuel salt	3.5 m/s	0.07 m/s
Maximum speed of the intermediate fluid (liquid lead)	1.75 m/s	0.035 m/s
Maximum speed of the intermediate fluid (salt)	5.5 m/s	0.11 m/s
Maximum temperature of the materials	700 °C	1 °C
Minimum margin to solidification of the fuel salt	50 °C	1 °C
Minimum margin to solidification of the intermediate fluid	40 °C	1 °C

Table 4: Main constrained parameters with their limiting value and acceptable deviation

When liquid lead is used as intermediate fluid, we notice that the gap between the plates on the fuel side is quite large, that implies also voluminous connecting parts. This fact is partially linked to the speed limitation for the lead flow. This also results in a higher temperature at the fuel entrance. When a salt fluid such as FLiNaK or NaF-NaBF₄ is used as intermediate fluid, the heat exchanger outlet temperature is higher which allows raising the thermodynamic yield. Nevertheless, the heat exchanger temperature drop is smaller in this case and high velocities are required. Nevertheless these quite high intermediate salt flow velocities seems not really acceptable because of the pumping performance and erosion problems. The 3 cases discussed here are only examples: changing the constraints to take into account technological data is possible and will produce other solutions.

Evaluated parameter	Pb	FLiNaK	NaF-NaBF ₄
Diameter of the fuel salt pipes [mm]	301	283	303
Diameter of the intermediate fluid pipes [mm]	897	507	470
Thickness of the plates [mm]	1.61	1.51	1.65
Fuel salt temperature at core entrance [°C]	754	698	704
Fuel salt temperature increase in the core [°C]	89	106	98
Intermediate fluid temperature increase within the heat exchangers [°C]	99	41	66
Mean temperature difference between the two fluids in the heat exchangers [°C]	382	242	280
Intermediate fluid temperature at the heat exchangers outlet [°C]	466	530	506
Thickness of the fuel salt channel [mm]	3.38	2.17	2.37
Thickness of the intermediate fluid channel [mm]	29.8	4.49	4.38
Fuel salt speed in the pipes [m/s]	3.92	3.97	3.73
Fuel salt speed in the heat exchangers [m/s]	3.85	2.36	2.91
Intermediate fluid speed in the pipes [m/s]	1.94	6.00	5.67
Intermediate fluid speed in the heat exchangers [m/s]	1.92	5.54	5.75
Maximum temperature of the intermediate fluid [°C]	523	622	595
Maximum temperature of the materials [°C]	701	701	699
Margin to the solidification of the fuel salt [°C]	43.7	54.7	46.7
Margin to the solidification of the intermediate fluid [°C]	39.6	34.5	56.2
Pressure loss of the fuel salt in the heat exchangers [bar]	2.56	2.03	2.56
Pressure loss of the fuel salt in the pipes [bar]	0.99	1.02	0.90
Pressure loss of the intermediate fluid in the heat exchangers [bar]	0.09	2.09	1.66
Pressure loss of the intermediate fluid in the pipes [bar]	0.32	0.71	0.57

Table 5: Typical sets of parameters evaluated for the three intermediate fluids considered

An example of the temperature distributions in the heat exchangers can be plotted as in Figure 3, in the case of liquid lead. At the top of the heat exchangers (hot fuel salt inlet and heated intermediate fluid outlet), the maximum salt temperature is significantly higher than that of the plate (labeled " T_{\max} material" in Fig 3). The salt's poor thermal conductivity functions as a protection for the heat exchanger plates during normal operation. The same holds at the bottom of the heat exchangers (cooled fuel salt outlet and cold intermediate fluid inlet) but here, the fuel salt temperature (labeled " T_{\min} salt") draws near to that of its solidification. Thus, it is, indeed, the lowest permissible fuel salt temperature that constrains the minimal plate surface temperature. On the intermediate fluid side, since lead becomes very corrosive beyond 500-550 °C, the maximum plate surface temperature has to be limited, thus lowering the output lead temperature (labeled " T_{\max} lead"). On the other hand, the lead solidification temperature constrains the lead input temperature (labeled " T_{\min} lead").

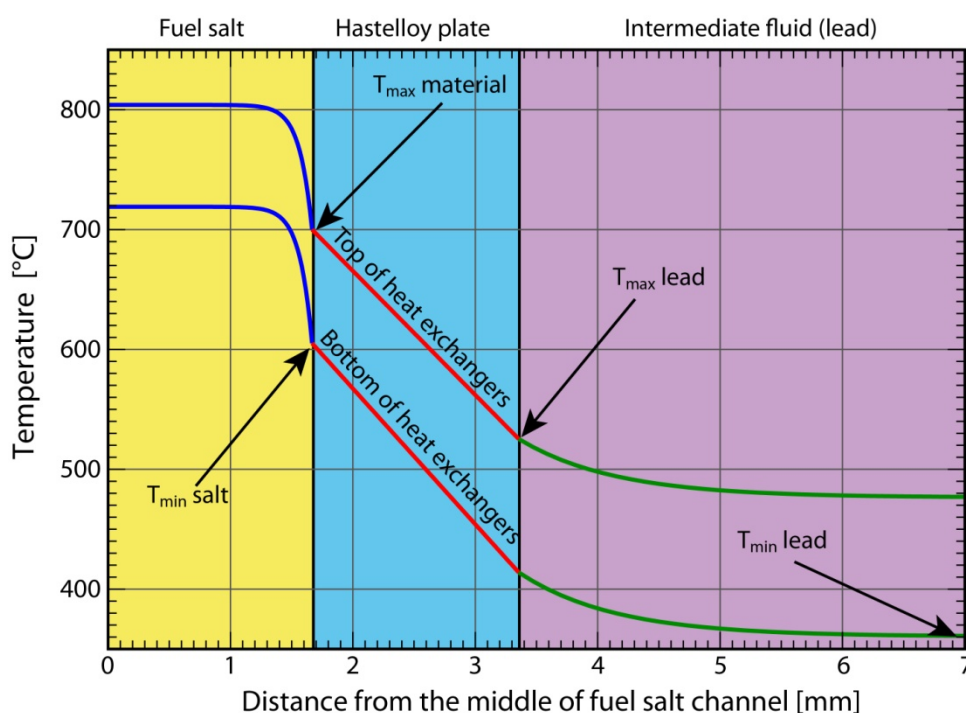


Fig 3. Qualitative representation of the temperature distributions in a heat exchanger

Four constrained temperatures limit the temperature ranges. It is mandatory that these temperature limits be observed at all times whatever the reactor's operating mode except, possibly, during rare short duration transient states (incidental or accidental occurrences).

Conclusions

This paper describes two design studies of the Molten Salt Fast Reactor, related to the fuel circuit, namely the choice of the fuel salt composition and a global study of the heat exchangers base on an approximate method developed to take into account the requirements of the entire fuel circuit, since the fuel salt is also used as the coolant in such reactors.

Concerning the choice of the liquid fuel, two types of salt have been studied: a fluoride or a chloride liquid salt. No discriminating difference between fluoride and chloride salts can be identified from a chemical standpoint: their characteristics are quite different but none is exclusionary. However, considering the neutronic standpoint, we demonstrate the real limited ability of the chloride salt to ensure breeding while used in a Thorium-based MSFR, together with the unavoidable production of significant amounts of the radiotoxic and unconfined ^{36}Cl and the irradiation damages in both cases. These studies demonstrate the definite advantage of using fluoride salts in a MSFR versus chloride salts.

Concerning the conceptual design of the fuel heat exchangers, the interdependence of all the reactor components requires a global analysis of the entire fuel circuit. An approximate method, which takes into account all the constraints presently known (physical, chemical, technological...) has been developed to ascertain whether solutions may exist for this multi-parameter problem. Examples of such solutions in the constraints phase have been shown here: these are only indicative but demonstrate that relevant configurations may be identified. These configurations are going to evolve according to new constraints as they appear. A more complete method, including more realistic models, will have to be developed to further assess the fuel circuit of such innovative reactors.

Acknowledgments

The authors wish to thank the PACEN (Programme sur l'Aval du Cycle et l'Energie Nucléaire) and NEEDS (Nucléaire : Energie, Environnement, Déchets, Société) programs of the French Centre National de la Recherche Scientifique (CNRS), the IN2P3 department of CNRS, and the European program EVOL (Evaluation and Viability of Liquid Fuel Fast Reactor System) of FP7 for their support. We are also very thankful to Elisabeth Huffer for her help during the translation of this paper and to Olivier Doche for his advice in some of the heat exchanger aspects.

References

- [1] L.Mathieu et al, ***“Possible Configurations for the TMSR and advantages of the Fast Non Moderated Version”***, Nuclear Science and Engineering 161, pp78–89 (2009)
- [2] E. Merle-Lucotte, D. Heuer, M. Allibert, M. Brovchenko, N. Capellan, and V. Ghetta, ***“Launching the Thorium Fuel Cycle with the Molten Salt Fast Reactor”***, Proceedings of the ICAPP'09 Conference, Paper 11190, Nice, France (2011)
- [3] E.Merle-Lucotte et al, ***“Simulation Tools and New Developments of the Molten Salt Fast Reactor”***, Proceedings of ENC2010, Paper A0115, Barcelona, Spain (2010)
- [4] S. Delpech, E. Merle-Lucotte, D. Heuer, M. Allibert, V. Ghetta, C. Le-Brun, L. Mathieu, G. Picard, ***“Reactor physics and reprocessing scheme for innovative molten salt reactor system”***, J. of Fluorine Chemistry, 130 Issue 1, p. 11-17 (2009)
- [5] E. Merle-Lucotte, D. Heuer et al, ***“Minimizing the Fissile Inventory of the Molten Salt Fast Reactor”***, Proceedings of the Advances in Nuclear Fuel Management IV (ANFM 2009) Conference, Hilton Head Island, USA (2009)
- [6] E. Merle-Lucotte, D. Heuer et al., ***“Optimizing the Burning Efficiency and the Deployment Capacities of the Molten Salt Fast Reactor”***, Proceedings of the International Conference Global 2009, Paper 9149, Paris, France (2009)
- [7] C.Renault et al, ***“The Molten Salt Reactor (MSR) in Generation IV: Overview and Perspectives”***, Proceedings of the GIF Symposium, France (2009)
- [8] M. Brovchenko, D. Heuer, E. Merle-Lucotte, M. Allibert, V. Ghetta, A. Laureau, ***“Preliminary safety calculations to improve the design of Molten Salt Fast Reactor”***, Proceedings of the PHYSOR 2012 International Conference, Knoxville, USA (2012)
- [9] A.-M. Bianchi, Y. Fautrelle et J. Etay, ***“Transferts thermiques”***, Presses polytechniques et universitaires romandes, pp 170 (2004)
- [10] V. Ignatiev, O. Feynberg, A. Merzlyakov et al., ***“Progress in Development of MOSART Concept with Th Support”***, Proceedings of ICAPP 2012, Paper 12394 Chicago, USA, (2012)
- [11] O. Benes, R.J.M. Konings, ***“Thermodynamic properties and phase diagrams of fluoride salts for nuclear applications”***, Journal of Fluorine Chemistry 130, pp 22-29 (2009)
- [12] <http://www.oecd-nea.org/science/reports/2007/nea6195-handbook.html>
- [13] D.J.Rogers, ***“Fusion Properties and Heat Capacities of the Eutectic LiF-NaF-KF Melt”***, Journal Chem. Eng. Data, 27 p.366-367 (1982)